Author(s): Ranta, Mikaela & Hinkkanen, Marko & Luomi, Jorma

Title: Inductance identification of an induction machine taking load-dependent saturation into account

Year: 2008

Version: Post print

**Please cite the original version:**

Ranta, Mikaela & Hinkkanen, Marko & Luomi, Jorma. 2008. Inductance identification of an induction machine taking load-dependent saturation into account. 18th International Conference on Electrical Machines, 2008. ICEM 2008. 6. ISBN 978-1-4244-1736-0 (electronic). DOI: 10.1109/icelmach.2008.4799920.

# Inductance Identification of an Induction Machine Taking Load-Dependent Saturation Into Account

Mikaela Ranta, Marko Hinkkanen, and Jorma Luomi
Helsinki University of Technology, Department of Electrical Engineering
P.O. BOX 3000, FI-02015 TKK, Finland
Email: mikaela.ranta@tkk.fi; marko.hinkkanen@tkk.fi; jorma.luomi@tkk.fi

***Abstract*—The paper proposes an identification method for the inductances of induction machines, based on signal injection. Due to magnetic saturation, a saturation-induced saliency appears in the induction motor, and the total leakage inductance estimate depends on the angle of the excitation signal. The proposed identification method is based on a small-signal model that includes the saturation-induced saliency. Because of the saturation, the load also affects the estimate, and measurements are needed in different operating points. Using the identified total leakage inductance, an estimate of the stator inductance can be obtained. The identification method is applied to computer simulations and laboratory experiments of a 2.2-kW induction motor.**

## I. Introduction

The control of an induction motor drive is based on a dynamic model of the motor. The parameters of the motor model are not known in advance, but have to be identified either off-line during the commissioning of the drive or on-line using an adaptation mechanism. The traditional way of identifying the parameters is to use no-load and locked-rotor tests. In practice, locking the rotor is usually not possible, but a similar test can be performed using high-frequency signal injection [1]. A number of algorithms have been developed for identifying the parameters of the motor based on these ideas, e.g. [2], [3], [4]. Numerous other types of identification methods, for instance various observer-based techniques, have also been developed [5].

The induction motor is usually designed to be magnetically saturated in the rated operating point. In many cases, the magnetizing inductance is assumed to be a function of the magnetizing current. The magnetizing curve can be identified by means of a series of no-load measurements. Due to the saturation, however, the magnetizing inductance is also affected by the rotor current [6], [7], particularly when the rotor slots are closed or skewed. Therefore, the results obtained using the no-load test hold only at light loads, i.e. when the rotor current is close to zero. As the load increases, and thus the rotor current increases, the magnetizing inductance and the rotor leakage inductance will change. Typical saturation characteristics of the magnetizing branch are shown in Fig. 1.

To obtain a value of the magnetizing inductance with a good accuracy, the inductance needs to be identified during the operation of the motor at different loads. The small-signal impedance can be measured using high-frequency signal injection, and the total leakage inductance can then be obtained. Based on this inductance and the operating-point data, it is also possible to estimate the load-dependent value of the magnetizing inductance [8]. Due to magnetic saturation, however, the impedance seen by the high-frequency signal depends on the direction of the excitation voltage signal [9], [10], giving rise to a saliency phenomenon. The identified value of the total leakage inductance is thus affected by the direction of the signal. The identification of the leakage inductance should, therefore, be based on a motor model taking into account the saturation phenomenon. Otherwise, incremental quantities might be obtained instead of the desired operating-point quantities.

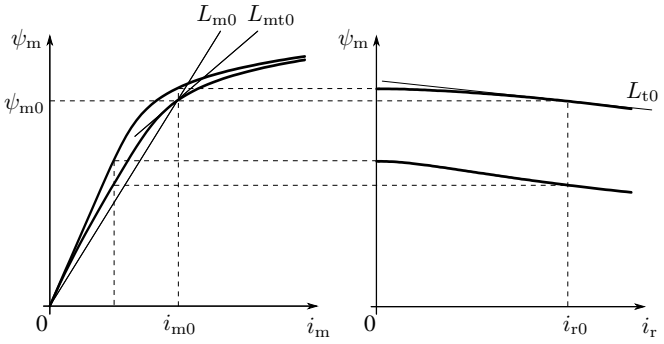


Fig. 1. Typical saturation characteristics of the main flux $\psi_{\mathrm{m}}(i_{\mathrm{m}}, i_{\mathrm{r}})$. On the left-hand side, the main flux is shown as a function of the magnetizing current $i_{\mathrm{m}}$: the upper curve corresponds to no-load operation (rotor current $i_{\mathrm{r}} = 0$) and the lower curve corresponds to operation under load ($i_{\mathrm{r}} = i_{\mathrm{r0}}$). On the right-hand side, the main flux is shown as a function of the rotor current at two different values of the magnetizing current: the upper curve corresponds to the magnetizing current $i_{\mathrm{m0}}$, and the lower curve corresponds to half of this value. The incremental inductances $L_{\mathrm{mt0}} = (\partial\psi_{\mathrm{m}}/\partial i_{\mathrm{m}})_0$ and $L_{\mathrm{t0}} = (\partial\psi_{\mathrm{m}}/\partial i_{\mathrm{r}})_0$, and the operating-point inductance $L_{\mathrm{m0}} = \psi_{\mathrm{m0}}/i_{\mathrm{m0}}$ are illustrated in the operating point $\psi_{\mathrm{m0}} = \psi_{\mathrm{m}}(i_{\mathrm{m0}}, i_{\mathrm{r0}})$.

This paper proposes an identification method based on the motor model presented in [11]. The total leakage inductance is obtained in different operating points by analyzing the response to high-frequency voltage injection. Both the saturation-induced saliency and the influence of load variations are considered in the identification. Based on the identified total leakage inductance, an estimate of the stator inductance is obtained. The identification method is applied to computer simulations and laboratory experiments of a 2.2-kW induction motor.

## II. Induction Motor Model

### A. Saturable Dynamic Model

In a reference frame rotating at the stator angular frequency $\omega_\mathrm{s}$, the induction motor can be described by

$$\frac{\mathrm{d}\boldsymbol{\psi}_\mathrm{s}}{\mathrm{d}t} = \boldsymbol{u}_\mathrm{s} - R_\mathrm{s}\boldsymbol{i}_\mathrm{s} - \omega_\mathrm{s}\mathbf{J}\boldsymbol{\psi}_\mathrm{s} \tag{1a}$$

$$\frac{\mathrm{d}\boldsymbol{\psi}_\mathrm{r}}{\mathrm{d}t} = -R_\mathrm{r}\boldsymbol{i}_\mathrm{r} - (\omega_\mathrm{s} - \omega_\mathrm{m})\,\mathbf{J}\boldsymbol{\psi}_\mathrm{r} \tag{1b}$$

where the stator voltage is denoted by $\boldsymbol{u}_\mathrm{s}$, the stator current by $\boldsymbol{i}_\mathrm{s}$, the rotor current by $\boldsymbol{i}_\mathrm{r}$, the stator flux linkage by $\boldsymbol{\psi}_\mathrm{s}$, and the rotor flux linkage by $\boldsymbol{\psi}_\mathrm{r}$. Real-valued space vectors are used, for example, the rotor current vector is $\boldsymbol{i}_\mathrm{r} = [i_\mathrm{rd}, i_\mathrm{rq}]^\mathrm{T}$ and its magnitude is $i_\mathrm{r} = \sqrt{i_\mathrm{rd}^2 + i_\mathrm{rq}^2}$. The stator and rotor resistances are denoted by $R_\mathrm{s}$ and $R_\mathrm{r}$, respectively. The electrical angular speed of the rotor is $\omega_\mathrm{m}$ and the angular slip frequency $\omega_\mathrm{r} = \omega_\mathrm{s} - \omega_\mathrm{m}$. The orthogonal rotation matrix, the identity matrix and the zero matrix are defined as

$$\mathbf{J} = \begin{bmatrix} 0 & -1 \\ 1 & 0 \end{bmatrix}, \quad \mathbf{I} = \begin{bmatrix} 1 & 0 \\ 0 & 1 \end{bmatrix}, \quad \mathbf{0} = \begin{bmatrix} 0 & 0 \\ 0 & 0 \end{bmatrix} \tag{2}$$

respectively. The stator and rotor fluxes are

$$\boldsymbol{\psi}_\mathrm{s} = L_\mathrm{s}\boldsymbol{i}_\mathrm{s} + L_\mathrm{m}\boldsymbol{i}_\mathrm{r}, \quad \boldsymbol{\psi}_\mathrm{r} = L_\mathrm{m}\boldsymbol{i}_\mathrm{s} + L_\mathrm{r}\boldsymbol{i}_\mathrm{r} \tag{3}$$

respectively, where $L_\mathrm{m}$ is the magnetizing inductance. Denoting the stator and rotor leakage inductances by $L_{\mathrm{s}\sigma}$ and $L_{\mathrm{r}\sigma}$, respectively, the stator inductance is $L_\mathrm{s} = L_\mathrm{m} + L_{\mathrm{s}\sigma}$ and the rotor inductance is $L_\mathrm{r} = L_\mathrm{m} + L_{\mathrm{r}\sigma}$.

In Fig. 1, typical saturation characteristics of the main flux $\psi_\mathrm{m}$ are shown. The main flux is shown both as a function of the magnetizing current $i_\mathrm{m}$, keeping the rotor current constant, and as a function of the rotor current $i_\mathrm{r}$, keeping the magnetizing current constant. The magnetizing and rotor leakage inductances are functions of both currents:

$$\begin{aligned} L_\mathrm{m}(i_\mathrm{m}, i_\mathrm{r}) &= \psi_\mathrm{m}(i_\mathrm{m}, i_\mathrm{r})/i_\mathrm{m} \\ L_{\mathrm{r}\sigma}(i_\mathrm{m}, i_\mathrm{r}) &= \psi_{\mathrm{r}\sigma}(i_\mathrm{m}, i_\mathrm{r})/i_\mathrm{r} \end{aligned} \tag{4}$$

respectively. The stator leakage inductance $L_{\mathrm{s}\sigma}$ is assumed to be constant for simplicity. Incremental inductances are defined by

$$L_\mathrm{mt} = \frac{\partial\psi_\mathrm{m}}{\partial i_\mathrm{m}}; \quad L_{\mathrm{r}\sigma\mathrm{t}} = \frac{\partial\psi_{\mathrm{r}\sigma}}{\partial i_\mathrm{r}}; \quad L_\mathrm{t} = \frac{\partial\psi_\mathrm{m}}{\partial i_\mathrm{r}} = \frac{\partial\psi_{\mathrm{r}\sigma}}{\partial i_\mathrm{m}} \tag{5}$$

where $L_\mathrm{t}$ is the mutual inductance between the magnetizing branch and the rotor leakage branch. The last equality is due to the reciprocity conditions of the model [11]. As seen in Fig. 1, the main flux decreases as the rotor current increases. Therefore, the mutual inductance $L_\mathrm{t}$ is negative.

### B. Small-Signal Model

Based on the induction motor model and the assumptions in (4), the small-signal model can be written as [11]

$$\frac{\mathrm{d}\tilde{\boldsymbol{x}}}{\mathrm{d}t} = \boldsymbol{A}\tilde{\boldsymbol{x}} + \boldsymbol{B}_\mathrm{s}\tilde{\boldsymbol{u}}_\mathrm{s} + \boldsymbol{b}\tilde{\omega}_\mathrm{m} \tag{6}$$

where tildes refer to deviations around the operating point. The state vector and the input matrices are

$$\tilde{\boldsymbol{x}} = \begin{bmatrix} \tilde{\boldsymbol{\psi}}_\mathrm{s} \\ \tilde{\boldsymbol{\psi}}_\mathrm{r} \end{bmatrix}, \quad \boldsymbol{B}_\mathrm{s} = \begin{bmatrix} \mathbf{I} \\ \mathbf{0} \end{bmatrix}, \quad \boldsymbol{b} = \begin{bmatrix} 0 \\ 0 \\ \mathbf{J}\boldsymbol{\psi}_{\mathrm{r}0} \end{bmatrix} \tag{7}$$

and the state matrix is given by

$$\boldsymbol{A} = -\begin{bmatrix} R_\mathrm{s}\mathbf{I} & \mathbf{0} \\ \mathbf{0} & R_\mathrm{r}\mathbf{I} \end{bmatrix}\boldsymbol{L}^{-1} - \begin{bmatrix} \omega_{\mathrm{s}0}\mathbf{J} & \mathbf{0} \\ \mathbf{0} & \omega_{\mathrm{r}0}\mathbf{J} \end{bmatrix} \tag{8}$$

where operating-point quantities are marked with the subscript 0. The inductance matrix is

$$\begin{aligned} \boldsymbol{L} = &\begin{bmatrix} L_{\mathrm{s}0}\mathbf{I} & L_{\mathrm{m}0}\mathbf{I} \\ L_{\mathrm{m}0}\mathbf{I} & L_{\mathrm{r}0}\mathbf{I} \end{bmatrix} \\ &+ \frac{L_{\mathrm{mt}0} - L_{\mathrm{m}0}}{i_{\mathrm{m}0}^2}\begin{bmatrix} \boldsymbol{i}_{\mathrm{m}0}\boldsymbol{i}_{\mathrm{m}0}^\mathrm{T} & \boldsymbol{i}_{\mathrm{m}0}\boldsymbol{i}_{\mathrm{m}0}^\mathrm{T} \\ \boldsymbol{i}_{\mathrm{m}0}\boldsymbol{i}_{\mathrm{m}0}^\mathrm{T} & \boldsymbol{i}_{\mathrm{m}0}\boldsymbol{i}_{\mathrm{m}0}^\mathrm{T} \end{bmatrix} \\ &+ \frac{L_{\mathrm{r}\sigma\mathrm{t}0} - L_{\mathrm{r}\sigma0}}{i_{\mathrm{r}0}^2}\begin{bmatrix} \mathbf{0} & \mathbf{0} \\ \mathbf{0} & \boldsymbol{i}_{\mathrm{r}0}\boldsymbol{i}_{\mathrm{r}0}^\mathrm{T} \end{bmatrix} \\ &+ \frac{L_{\mathrm{t}0}}{i_{\mathrm{m}0}i_{\mathrm{r}0}}\begin{bmatrix} \mathbf{0} & \boldsymbol{i}_{\mathrm{m}0}\boldsymbol{i}_{\mathrm{r}0}^\mathrm{T} \\ \boldsymbol{i}_{\mathrm{r}0}\boldsymbol{i}_{\mathrm{m}0}^\mathrm{T} & \boldsymbol{i}_{\mathrm{m}0}\boldsymbol{i}_{\mathrm{r}0}^\mathrm{T} + \boldsymbol{i}_{\mathrm{r}0}\boldsymbol{i}_{\mathrm{m}0}^\mathrm{T} \end{bmatrix} \end{aligned} \tag{9}$$

The last three terms in the inductance matrix are due to the saturation.

The small-signal impedance relating the current to the voltage, $\tilde{\boldsymbol{u}}_\mathrm{s}(s) = \boldsymbol{Z}_\mathrm{s}(s)\tilde{\boldsymbol{i}}_\mathrm{s}(s)$, can be written as

$$\boldsymbol{Z}_\mathrm{s}(s) = \begin{bmatrix} Z_\mathrm{dd}(s) & Z_\mathrm{dq}(s) \\ Z_\mathrm{qd}(s) & Z_\mathrm{qq}(s) \end{bmatrix} = \left[\boldsymbol{C}_\mathrm{s}\left(s\mathbf{I} - \boldsymbol{A}\right)^{-1}\boldsymbol{B}_\mathrm{s}\right]^{-1} \tag{10}$$

where $\boldsymbol{C}_\mathrm{s} = \begin{bmatrix} \mathbf{I} & \mathbf{0} \end{bmatrix}\boldsymbol{L}^{-1}$. The inductance matrix and thus also the small-signal impedance are dependent on the directions of the operating-point magnetizing current and the operating-point rotor current. Hence, the saturation causes saliency for small-signal quantities.

### C. Reduced-Order Small-Signal Model

At higher injection frequencies, the deviations in the rotor flux and rotor speed may be omitted, resulting in a reduced-order small-signal model. The small-signal impedance can be written as

$$\boldsymbol{Z}_\mathrm{s}(s) = \boldsymbol{R}_\sigma + (s\mathbf{I} + \omega_{\mathrm{s}0}\mathbf{J})\,\boldsymbol{L}_\sigma \tag{11}$$

Due to the saturation, both the total leakage inductance $\boldsymbol{L}_\sigma$ and the total resistance $\boldsymbol{R}_\sigma$ are matrices depending on the directions of the operating-point currents $\boldsymbol{i}_{\mathrm{m}0}$ and $\boldsymbol{i}_{\mathrm{r}0}$ [11].

For the purpose of identification, the model in (11) can be simplified. Assuming that the saturation in the main flux and the mutual saturation do not influence the small-signal characteristics, i.e. $L_{\mathrm{mt}0} = L_{\mathrm{m}0}$ and $L_{\mathrm{t}0} = 0$, the total leakage inductance and the total resistance are

$$\begin{aligned} \boldsymbol{L}_\sigma &= \mathrm{e}^{\vartheta_{\mathrm{r}0}\mathbf{J}}\begin{bmatrix} L_{\sigma\mathrm{t}0} & 0 \\ 0 & L_{\sigma0} \end{bmatrix}\mathrm{e}^{-\vartheta_{\mathrm{r}0}\mathbf{J}} \\ \boldsymbol{R}_\sigma &= \mathrm{e}^{\vartheta_{\mathrm{r}0}\mathbf{J}}\begin{bmatrix} R_{\sigma\mathrm{t}0} & 0 \\ 0 & R_{\sigma0} \end{bmatrix}\mathrm{e}^{-\vartheta_{\mathrm{r}0}\mathbf{J}} \end{aligned} \tag{12}$$

respectively, where the angle of the operating-point rotor current is $\vartheta_{\mathrm{r}0}$ in the reference frame used. In this simplified

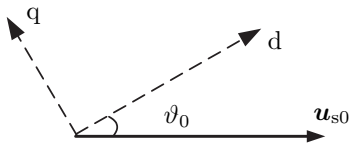


Fig. 2. Definition of the reference-frame angle $\vartheta_0$ used in the identification.

model, the inductance and resistance matrices do not depend on the angle of the magnetizing current. The impedance of the simplified model is

$$\boldsymbol{Z}_{\mathrm{s}}(s) = \mathrm{e}^{\vartheta_{\mathrm{r}0}\mathbf{J}} \begin{bmatrix} R_{\sigma\mathrm{t}0} + sL_{\sigma\mathrm{t}0} & -\omega_{\mathrm{s}0}L_{\sigma0} \\ \omega_{\mathrm{s}0}L_{\sigma\mathrm{t}0} & R_{\sigma0} + sL_{\sigma0} \end{bmatrix} \mathrm{e}^{-\vartheta_{\mathrm{r}0}\mathbf{J}} \quad (13)$$

where the operating-point total leakage inductance and resistance are

$$L_{\sigma0} = L_{\mathrm{s}\sigma} + k_{\mathrm{r}0}L_{\mathrm{r}\sigma0}, \quad R_{\sigma0} = R_{\mathrm{s}} + k_{\mathrm{r}0}^2 R_{\mathrm{r}} \quad (14)$$

respectively, and the incremental parameters are

$$L_{\sigma\mathrm{t}0} = L_{\mathrm{s}\sigma} + k_{\mathrm{rt}0}L_{\mathrm{r}\sigma\mathrm{t}0}, \quad R_{\sigma\mathrm{t}0} = R_{\mathrm{s}} + k_{\mathrm{rt}0}^2 R_{\mathrm{r}} \quad (15)$$

The magnetic coupling factors are $k_{\mathrm{r}0} = L_{\mathrm{m}0}/L_{\mathrm{r}0}$ and $k_{\mathrm{rt}0} = L_{\mathrm{m}0}/(L_{\mathrm{m}0} + L_{\mathrm{r}\sigma\mathrm{t}0})$. These coupling factors depend on the saturation, and the inductances and resistances in (13) depend on the coupling factors.

## III. Parameter Identification

### A. Total Leakage Inductance Identification

The small-signal impedance can be measured by means of high-frequency signal injection. Injecting a sinusoidal voltage signal first in the d direction and then in the q direction, all elements in the impedance matrix can be calculated. Assuming that the d axis is aligned with the operating-point rotor current, i.e. $\vartheta_{\mathrm{r}0} = 0$, the parameters in (13) can be obtained by[1]

$$\begin{aligned} L_{\sigma0} &= \mathrm{Im}\{Z_{\mathrm{qq}}\}/\omega_{\mathrm{c}}, \quad L_{\sigma\mathrm{t}0} = \mathrm{Im}\{Z_{\mathrm{dd}}\}/\omega_{\mathrm{c}} \\ R_{\sigma0} &= \mathrm{Re}\{Z_{\mathrm{qq}}\}, \quad R_{\sigma\mathrm{t}0} = \mathrm{Re}\{Z_{\mathrm{dd}}\} \end{aligned} \quad (16)$$

where $\omega_{\mathrm{c}}$ is the angular frequency of the injection signal.

The angle of the rotor current is normally not known in advance. To overcome this problem, the parameters are identified in different reference frames. The impedance is measured in a reference frame aligned with the operating-point stator voltage. Denoting this impedance by $\boldsymbol{Z}'_{\mathrm{s}}$, the impedance in a reference frame having the angle $\vartheta_0$ with respect to the operating-point stator voltage $\boldsymbol{u}_{\mathrm{s}0}$ is calculated by

$$\boldsymbol{Z}_{\mathrm{s}}(s) = \mathrm{e}^{-\vartheta_0\mathbf{J}}\boldsymbol{Z}'_{\mathrm{s}}(s)\mathrm{e}^{\vartheta_0\mathbf{J}} \quad (17)$$

In this manner, estimates of the parameters are obtained as a function of the reference-frame angle $\vartheta_0$ illustrated in Fig. 2.

According to (13),

$$\mathrm{Im}\{Z_{\mathrm{qq}}\} = \omega_{\mathrm{c}}[L_{\sigma0}\cos^2(\vartheta_{\mathrm{r}0}) + L_{\sigma\mathrm{t}0}\sin^2(\vartheta_{\mathrm{r}0})] \quad (18)$$

[1]The inductances could alternatively be calculated as $L_{\sigma0} = -\mathrm{Re}\{Z_{\mathrm{dq}}\}/\omega_{\mathrm{s}0}$ and $L_{\sigma\mathrm{t}0} = \mathrm{Re}\{Z_{\mathrm{qd}}\}/\omega_{\mathrm{s}0}$.

In the case of no saturation, $L_{\sigma\mathrm{t}0} = L_{\sigma0}$, and the measured impedance is not dependent on the angle of the operating-point rotor current. As the motor saturates, the incremental inductance $L_{\sigma\mathrm{t}0} < L_{\sigma0}$. It can be seen in (18) that the maximum value of the impedance $\mathrm{Im}\{Z_{\mathrm{qq}}\}$ equals $\omega_{\mathrm{c}}L_{\sigma0}$ and the minimum value equals $\omega_{\mathrm{c}}L_{\sigma\mathrm{t}0}$. Therefore, the maximum value of the impedance should be chosen for estimating $L_{\sigma0}$. The other parameters can then also be identified at the same angle value.

### B. Stator Inductance Identification

In steady state, the stator flux can be calculated based on the operating-point stator voltage and stator current according to

$$\boldsymbol{\psi}_{\mathrm{s}0} = -\mathbf{J}(\boldsymbol{u}_{\mathrm{s}0} - R_{\mathrm{s}}\boldsymbol{i}_{\mathrm{s}0})/\omega_{\mathrm{s}0} \quad (19)$$

The stator inductance can then be obtained by [8]

$$L_{\mathrm{s}0} = \frac{\psi_{\mathrm{s}0}^2 - L_{\sigma0}\boldsymbol{i}_{\mathrm{s}0}^{\mathrm{T}}\boldsymbol{\psi}_{\mathrm{s}0}}{\boldsymbol{i}_{\mathrm{s}0}^{\mathrm{T}}\boldsymbol{\psi}_{\mathrm{s}0} - L_{\sigma0}i_{\mathrm{s}0}^2} \quad (20)$$

The stator inductance can thus be identified based on operating-point data and the total leakage inductance $L_{\sigma0}$ identified by means of signal injection. The operating-point magnetizing inductance is $L_{\mathrm{m}0} = L_{\mathrm{s}0} - L_{\mathrm{s}\sigma}$.

### C. Identification Errors Caused by Approximations

*1) Saturation:* The simplified model (13) includes the saturation in the rotor leakage flux as a function of the rotor current, but the saturation in the main flux ($L_{\mathrm{mt}0} = L_{\mathrm{m}0}$) and the mutual saturation ($L_{\mathrm{t}0} = 0$) between the main flux and the rotor leakage flux are not included in the small-signal model. The impedance matrix becomes complicated if these parameters are included, and it is difficult to analyze the influence of the approximations analytically. Therefore, the influence of the approximations on the impedance was analyzed numerically in different operating points and for different injection frequencies using the data of a 2.2-kW motor.

According to the numerical analysis, the mutual inductance $L_{\mathrm{t}0}$ mainly affects the impedance element $Z_{\mathrm{dd}}$ and the real part of $Z_{\mathrm{qq}}$ in a reference frame aligned with the operating-point rotor current. As $L_{\sigma\mathrm{t}0}$, $R_{\sigma\mathrm{t}0}$ and $R_{\sigma0}$ are obtained from these elements, the approximation $L_{\mathrm{t}0} = 0$ may cause inaccuracies in the identified values of these parameters.

The numerical analysis also shows that the approximation $L_{\mathrm{mt}0} = L_{\mathrm{m}0}$ can lead to significant errors in the identified total leakage inductance. To better understand the influence of this parameter, analytical expressions were derived for the inductance matrix $\boldsymbol{L}_{\sigma}$ making only the approximation $L_{\mathrm{t}0} = 0$. When $L_{\mathrm{mt}0}$ is included, the inductance matrix is not only dependent on the angle of the rotor current, but also on the angle of the magnetizing current.

Two special cases appear in a reference frame aligned with the rotor current. If the angle of the operating-point magnetizing current is 90°, the inductance matrix (12) becomes

$$\boldsymbol{L}_{\sigma} = \begin{bmatrix} L_{\sigma\mathrm{t}0} & 0 \\ 0 & L_{\mathrm{s}\sigma} + k'_{\mathrm{r}0}L_{\mathrm{r}\sigma0} \end{bmatrix} \quad (21)$$

where the coupling factor is $k'_{\mathrm{r}0} = L_{\mathrm{mt}0}/(L_{\mathrm{mt}0} + L_{\mathrm{r}\sigma 0})$. If the angle between the currents is $0^\circ$ or $180^\circ$, the inductance matrix is

$$\boldsymbol{L}_\sigma = \begin{bmatrix} L_{\mathrm{s}\sigma} + k'_{\mathrm{rt}0} L_{\mathrm{r}\sigma\mathrm{t}0} & 0 \\ 0 & L_{\sigma 0} \end{bmatrix} \tag{22}$$

where the coupling factor $k'_{\mathrm{rt}0} = L_{\mathrm{mt}0}/(L_{\mathrm{mt}0} + L_{\mathrm{r}\sigma\mathrm{t}0})$.

The angle between the operating-point rotor current and the magnetizing current is normally close to $90^\circ$, and the measured inductance matrix is thus approximately given by (21). As the main flux saturates, $k'_{\mathrm{r}0} \neq k_{\mathrm{r}0}$, and the identified value of the leakage inductance deviates from the actual value of $L_{\sigma 0}$. If the rotor leakage inductance $L_{\mathrm{r}\sigma 0}$ is small compared to the incremental inductance $L_{\mathrm{mt}0}$, the influence of the main flux saturation is small as $k'_{\mathrm{r}0} \approx k_{\mathrm{r}0}$. However, significant errors may occur if the difference between $L_{\mathrm{mt}0}$ and $L_{\mathrm{m}0}$ is large and $L_{\mathrm{r}\sigma 0}$ is of the same order of magnitude as $L_{\mathrm{mt}0}$. The more the angle between the operating-point rotor current and the magnetizing current deviates from $90^\circ$, the smaller is the error in the leakage inductance.

The incremental magnetizing inductance has a similar influence on the resistance $R_{\sigma 0}$ as on the inductance $L_{\sigma 0}$. Due to the saturation in the main flux, the identified value of the resistance $R_{\sigma 0}$ is slightly smaller than the actual value.

*2) Skin Effect:* The skin effect is not taken into account in the identification. Due to the skin effect, the rotor leakage inductance observed at high frequencies is lower than the rotor leakage inductance at zero frequency, and the rotor resistance at high frequencies is higher than that at zero frequency. Assuming rectangular rotor bars with depth $d$, the rotor resistance and the rotor leakage inductance at angular frequency $\omega$ are [12]

$$R_{\mathrm{r}} = \frac{d}{\delta} \frac{\sinh(2d/\delta) + \sin(2d/\delta)}{\cosh(2d/\delta) - \cos(2d/\delta)} R_{\mathrm{r,dc}} \tag{23}$$

$$L_{\mathrm{r}\sigma} = \frac{3\delta}{2d} \frac{\sinh(2d/\delta) - \sin(2d/\delta)}{\cosh(2d/\delta) - \cos(2d/\delta)} L_{\mathrm{r}\sigma,\mathrm{dc}} \tag{24}$$

respectively, where the subscript dc marks the zero-frequency values, $\delta = \sqrt{2/(\omega\mu_0\sigma)}$ is the skin depth, $\mu_0$ being the permeability of free space and $\sigma$ the conductivity of the rotor bars. The behavior of the rotor leakage inductance and the rotor resistance as a function of the injection frequency is shown in Fig. 3. The skin effect has more influence on the resistance than on the inductance. In order to avoid large errors due to the skin effect, a low injection frequency should be chosen. On the other hand, the high-frequency approximation (11) does not hold if the injection frequency is too low.

## IV. Simulation Results

In order to investigate the parameter identification of the simplified model in (13), simulations were carried out in the Matlab/Simulink environment using the data of a 2.2-kW four-pole induction motor with skewed and closed rotor slots. The rated voltage of the motor is 400 V and the rated frequency 50 Hz. The stator leakage inductance was assumed to be constant while the magnetizing inductance and the rotor leakage inductance were modeled as functions of the magnetizing flux and the rotor leakage flux, i.e. $L_{\mathrm{m}}(\psi_{\mathrm{m}}, \psi_{\mathrm{r}\sigma})$ and $L_{\mathrm{r}\sigma}(\psi_{\mathrm{m}}, \psi_{\mathrm{r}\sigma})$ [13]. The inductance values were obtained from time-harmonic finite element analysis according to [14]. The skin effect and the iron losses were omitted in the simulation model.

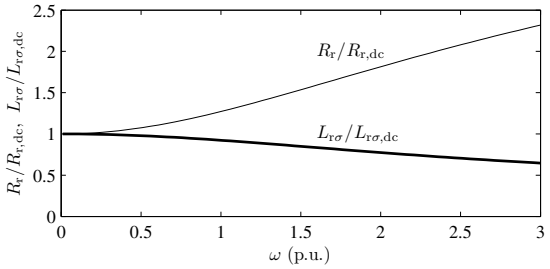


Fig. 3. Rotor resistance (23) and rotor leakage inductance (24) as a function of angular frequency $\omega$ when the depth of the rotor bar is 16 mm.

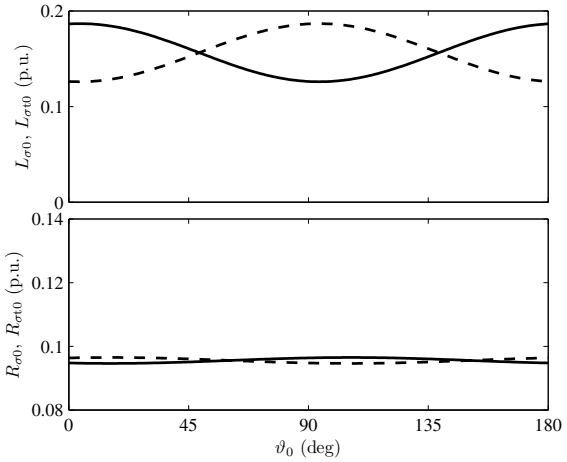


Fig. 4. Identified parameters based on the simulation data as a function of the reference-frame angle $\vartheta_0$ at zero speed. The slip frequency and the stator current are equal to their rated values. The injection frequency is 2.8 p.u. Operating-point quantities are shown by the solid lines and incremental quantities by the dashed lines.

The parameters were first identified at zero speed. The stator frequency was equal to the rated slip frequency and the stator current was equal to the rated current. The injection frequency was 1.2 p.u. (60 Hz) and the amplitude of the injected voltage 0.02 p.u. The identified parameters as a function of the reference-frame angle $\vartheta_0$ are shown in Fig. 4. The identified parameters and the actual parameters obtained from the simulation data are shown in Table I. For comparison, the total leakage inductance $L_{\sigma 0}$ and the resistance $R_{\sigma 0}$ were also identified using a conventional method in which rotating signal injection is used and the incremental inductances are assumed to be equal to the operating-point inductances [1]. At zero speed and rated slip frequency, the error in the total leakage inductance of the proposed method is only 1.6%, leading to an error of 0.9% in the stator inductance. When using the conventional method, the corresponding errors are 20% and 10.4%, respectively.

Next, the operating-point stator voltage was varied and the total leakage inductance and the stator inductance were

TABLE I
IDENTIFIED PARAMETERS FROM SIMULATIONS

| | Identified (p.u.) | | Actual (p.u.) |
|---|---|---|---|
| | Conventional | Proposed | |
| $L_{\sigma 0}$ | 0.152 | 0.187 | 0.190 |
| $L_{\sigma \mathrm{t}0}$ | | 0.126 | 0.129 |
| $R_{\sigma 0}$ | 0.099 | 0.095 | 0.097 |
| $R_{\sigma \mathrm{t}0}$ | | 0.096 | 0.099 |
| $L_{\mathrm{s}0}$ | 2.07 | 2.29 | 2.31 |

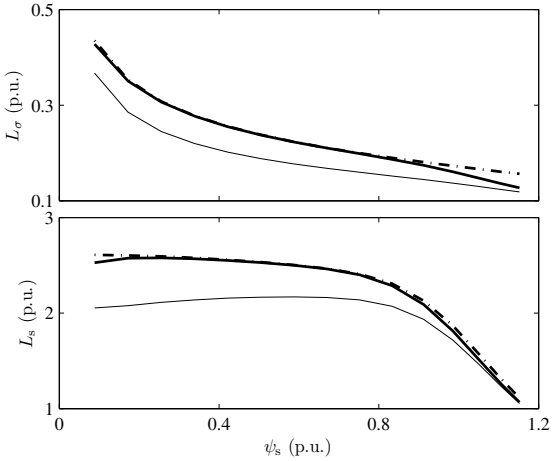


Fig. 5. Total leakage inductance and stator inductance as a function of the stator flux. Identified values obtained by the proposed method are shown by thick solid lines, values obtained by the conventional method are shown by thin solid lines and actual values by dash-dotted lines. The rotor speed is zero and the stator frequency equals the rated slip frequency.

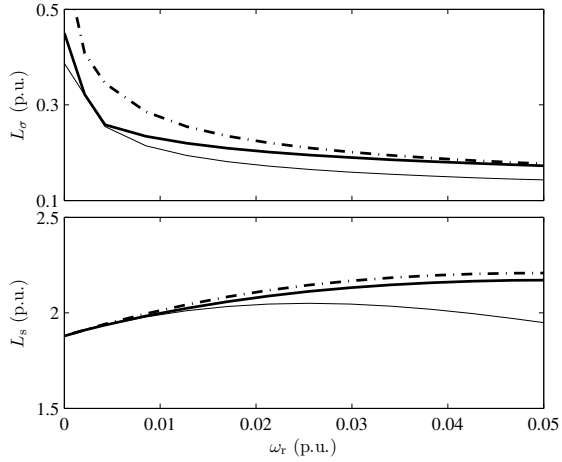


Fig. 6. Identified total leakage inductance and stator inductance as a function of the angular slip frequency as the stator frequency is 0.5 p.u. The rated angular slip frequency is 0.043 p.u. The parameters from the proposed method are shown by the thick solid lines, and the parameters from the conventional method by the thin solid lines. The dash-dotted lines show the actual values.

TABLE II
IDENTIFIED PARAMETERS FROM MEASUREMENTS

| | Conventional (p.u.) | Proposed (p.u.) |
|---|---|---|
| $L_{\sigma 0}$ | 0.138 | 0.149 |
| $L_{\sigma \mathrm{t}0}$ | | 0.130 |
| $R_{\sigma 0}$ | 0.114 | 0.118 |
| $R_{\sigma \mathrm{t}0}$ | | 0.111 |
| $L_{\mathrm{s}0}$ | 1.79 | 1.83 |

identified at different flux levels. The identified inductances are shown in Fig. 5 as a function of the stator flux. The stator flux was calculated using (19). The identified values are equal to the actual values at low values of the stator flux. As the stator flux increases above 0.8 p.u., an error can be observed in the total leakage inductance. Due to the saturation in the main flux, the identified value of the total leakage inductance is lower than the actual value. The corresponding error in the stator inductance is less than 5%. When using the conventional method, the error in the total leakage inductance is about 20% at all flux levels, and the error in the stator inductance is large at low flux levels. Similar simulations were carried out for a stator frequency of 0.5 p.u. and rated slip frequency. The behavior of the identified inductances as a function of the stator flux is practically identical to the behavior at zero speed.

The parameters were also identified at different torque values at the stator frequency of 0.5 p.u. and stator voltage of 0.5 p.u. The identified total leakage inductance and stator inductance are shown as a function of the angular slip frequency in Fig. 6. The accuracy of the proposed method is good at high loads, but at low loads, the identification error in the total leakage inductance increases. At low loads, the difference between the incremental magnetizing inductance and the operating-point magnetizing inductance is rather large, and the rotor leakage inductance is also relatively large, leading to a significant difference between $k'_{\mathrm{r}0}$ and $k_{\mathrm{r}0}$. To obtain a better estimate of the inductance, the influence of the main flux saturation on the small-signal characteristics should be taken into account. The error of the conventional method is rather large at all load values. At high loads, the error in the total leakage inductance leads to a large error in the stator inductance.

## V. EXPERIMENTAL RESULTS

In the laboratory experiments, a 2.2-kW induction motor was fed by a frequency converter controlled by a dSpace DS1103 PPC/DSP board. The parameters were first identified as the rotor was locked. The stator resistance was measured in advance for the calculation of the stator inductance and the stator flux. The same operating point was used as in the simulations, i.e. the stator frequency was equal to the rated slip frequency and the stator current was equal to the rated current. The identified parameters are shown in Fig. 7 as a function of the reference-frame angle $\vartheta_0$, and the identified parameters are presented in Table II. The conventional method [1] was also used for identification. As in the simulations, a smaller value is obtained for the total leakage inductance with the conventional method.

Measurements were also performed at the stator frequency 0.5 p.u. and rated slip frequency. The stator voltage was varied to obtain the inductances as functions of the stator flux in the same manner as in the simulations. The identified total leakage inductance and stator inductance are shown in

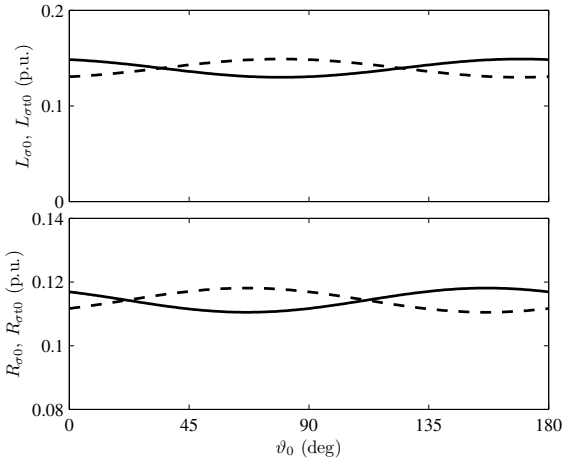


Fig. 7. Identified parameters based on the measured data as a function of the reference-frame angle $\vartheta_0$ at zero speed. The stator frequency equals the rated slip frequency, and the stator current equals the rated current. Operating-point quantities are shown by the solid lines and incremental quantities by the dashed lines.

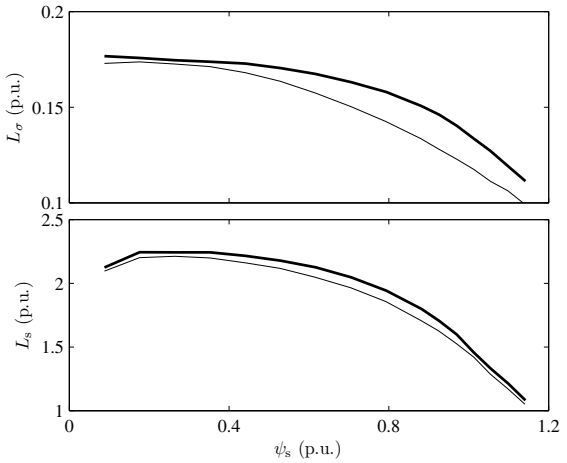


Fig. 8. Identified total leakage inductance and stator inductance obtained from the measured data. Values obtained by the proposed method are shown by thick solid lines and values obtained by the conventional method by thin solid lines. The stator frequency is 0.5 p.u. and the slip frequency equals its rated value.

Fig. 8. It is seen that the leakage inductance obtained by the conventional method is smaller than the inductance obtained by the proposed method at all flux levels.

## VI. Conclusions

Due to magnetic saturation, the small-signal impedance of an induction motor depends on the direction of the signal. This saliency phenomenon appears in the small-signal model if the dynamic model of the motor is properly linearized, and it can be used for developing improved parameter identification methods.

This paper proposes a method for the identification of the total leakage inductance, based on including the saturation of the rotor leakage inductance in the small-signal model. Sinusoidal voltage signal injection is applied in two perpendicular directions in order to take the saliency phenomenon into account. The angle of the rotor current needs not to be known in advance if the maximum value of the estimated total leakage inductance is selected in each operating point. Based on the identified value of the total leakage inductance and on operating-point data, an estimate is also obtained for the stator inductance.

The identification method was investigated by means of simulations and laboratory experiments. The results show that the identification accuracy is considerably improved as compared to a previously used method that is based on rotating signal injection. It could also be possible to include the effect of main-flux saturation and the skin effect in rotor conductors in the small-signal model used for parameter identification, which is a suitable topic for future research.

## Acknowledgement

The authors gratefully acknowledge ABB Oy for the financial support and Mr. Toni Tuovinen for the implementation of fitting algorithms.

## References

[1] D. Holliday, T. C. Green, and B. W. Williams, "On-line measurement of induction machine stator and rotor winding parameters," in *Proc. IEE PEVD Conf.*, London, U.K., Oct. 1994, pp. 485–469.

[2] M. Sumner and G. M. Asher, "Autocommissioning for voltage-referenced voltage-fed vector-controlled induction motor drives," *IEE Proc. B, Electr. Power Appl.*, vol. 140, no. 3, pp. 187–200, May 1993.

[3] S. Mao and T. C. Green, "DSP based on-line parameter identification of induction machine," in *Proc. IEE PEVD Conf.*, Nottingham, UK, Sept. 1996, pp. 48–53.

[4] R. J. Kerkman, J. D. Thunes, T. M. Rowan, and D. W. Schlegel, "A frequency-based determination of transient inductance and rotor resistance for field commissioning purposes," *IEEE Trans. Ind. Appl.*, vol. 32, no. 3, pp. 577–584, May/June 1996.

[5] H. A. Toliyat, E. Levi, and M. Raina, "A review of RFO induction motor parameter estimation techniques," *IEEE Trans. Energy Convers.*, vol. 18, no. 2, pp. 271–283, June 2003.

[6] A. Yahiaoui and F. Bouillault, "Saturation effect on the electromagnetic behaviour of an induction machine," *IEEE Trans. Magn.*, vol. 31, no. 3, pp. 2036–2039, May 1995.

[7] C. Gerada, K. Bradley, M. Sumner, and P. Sewell, "Evaluation and modelling of cross saturation due to leakage flux in vector controlled induction machines," in *Proc. IEEE IEMDC'03*, vol. 3, San Diego, CA, June 2003, pp. 1983–1989.

[8] J. L. Zamora and A. García-Cerrada, "Online estimation of the stator parameters in an induction motor using only voltage and current measurements," *IEEE Trans. Ind. Appl.*, vol. 36, no. 3, pp. 805–816, May/June 2000.

[9] V. Staudt, "Measuring differential inductances of asynchronous machines," *Euro. Trans. Electr. Power*, vol. 4, no. 1, pp. 27–33, Jan./Feb. 1994.

[10] M. L. Aime, M. W. Degner, and R. D. Lorenz, "Saturation measurements in AC machines using carrier signal injection," in *Conf. Rec. IEEE-IAS Annu. Meeting*, vol. 1, St. Louis, MO, Oct. 1998, pp. 159–166.

[11] M. Hinkkanen, A.-K. Repo, M. Cederholm, and J. Luomi, "Small-signal modelling of saturated induction machines with closed or skewed rotor slots," in *Conf. Rec. IEEE-IAS Annu. Meeting*, New Orleans, LA, Sept. 2007, pp. 1200–1206.

[12] P. L. Alger, *The Nature of Induction Machines*. New York: Gordon and Breach, 1965.

[13] T. Tuovinen, M. Hinkkanen, and J. Luomi, "Modeling of mutual saturation in induction machines," in *Conf. Rec. IEEE-IAS Annu. Meeting*, Edmonton, Canada, Oct. 2008, in press.

[14] A. Arkkio, "Analysis of induction motors based on the numerical solution of the magnetic field and circuit equations," Ph.D. dissertation, Dept. Elect. Commun. Eng., Helsinki Univ. Tech., Espoo, Finland, Dec. 1987.